Subretinal Glial Membranes in Eyes With Geographic Atrophy

Malia M. Edwards, D. Scott McLeod, Imran A. Bhutto, Rhonda Grebe, Maeve Duffy, and Gerard A. Lutty

Department of Ophthalmology, Wilmer Eye Institute, Johns Hopkins University School of Medicine, Baltimore, Maryland, United States

Correspondence: Malia M. Edwards, The Wilmer Eye Institute, M023 Smith Building, Johns Hopkins Hospital, 400 North Broadway, Baltimore, MD 21287-9115, USA; medwar28@jhmi.edu.

Submitted: December 2, 2016
Accepted: January 31, 2017

Citation: Edwards MM, McLeod DS, Bhutto IA, Grebe R, Duffy M, Lutty GA. Subretinal glial membranes in eyes with geographic atrophy. *Invest Ophthalmol Vis Sci*. 2017;58:1352–1367. DOI:10.1167/iovs.16-21229

Purpose. Müller cells create the external limiting membrane (ELM) by forming junctions with photoreceptor cells. This study evaluated the relationship between focal photoreceptors and RPE loss in geographic atrophy (GA) and Müller cell extension into the subretinal space.

Methods. Human donor eyes with no retinal disease or geographic atrophy (GA) were fixed and the eye cups imaged. The retinal posterior pole was stained for glial fibrillary acidic protein (GFAP; astrocytes and activated Müller cells) and vimentin (Müller cells) while the submacular choroids were labeled with Ulex Europaeus Agglutinin lectin (blood vessels). Choroids and retinas were imaged using a Zeiss 710 confocal microscope. Additional eyes were cryopreserved or processed for transmission electron microscopy (TEM) to better visualize the Müller cells.

Results. Vimentin staining of aged control retinas ($n = 4$) revealed a panretinal cobblestone-like ELM. While this pattern was also observed in the GA retinas ($n = 7$), each also had a distinct area in which vimentin$^+$ and vimentin$^+$/GFAP$^+$ processes created a subretinal membrane. Subretinal glial membranes closely matched areas of RPE atrophy in the gross photos. Choroidal vascular loss was also evident in these atrophic areas. Smaller glial projections were noted, which correlated with drusen in gross photos. The presence of glia in the subretinal space was confirmed by TEM and cross cross-section immunohistochemistry.

Conclusions. In eyes with GA, subretinal Müller cell membranes present in areas of RPE atrophy may be a Müller cell attempt to replace the ELM. These membranes could interfere with treatments such as stem cell therapy.

Keywords: Müller cells, glia, AMD, geographic atrophy

Müller cells, the primary glial cell of the retina, span the entire retinal thickness and are identified by vimentin and glutamine synthetase (GS). Müller cell endfeet bind to the internal limiting membrane (ILM),[1] separating the retina and vitreous while their posterior processes form adhesion junctions with photoreceptors to create the external limiting membrane (ELM). These glial cells provide the retinal suprastructure and interact with most retinal cell types. They also maintain ion homeostasis, synthesize glutamine, and assist in synaptic activity.[2] Müller cells respond rapidly to injury by increasing their glial fibrillary acidic protein (GFAP) expression and taking on a reactive state.

Despite neuronal dependence on Müller cells and astrocytes, very little is known about their role in retinal diseases, such as AMD. Geographic atrophy (GA), the advanced dry form of AMD, is characterized by the loss of RPE cells and subsequent dropout of choroidal vessels.[3,4] Müller cells above drusen and/or RPE and photoreceptor loss are known to express GFAP.[5–8] Focal areas of GFAP accumulation in the outer nuclear layer (ONL) have also been reported anterior to drusen in retinas with GA.[5,8] Interestingly, Müller cells migrate toward the ELM when proliferating and this migration is crucial to Müller cell remodeling and dedifferentiation that takes place in other animals.[9] Therefore, glial remodeling in AMD could contribute to the Müller cell accumulation at the ELM. The idea of remodeling is supported by our recent report that Müller cells and astrocytes form membranes on the vitreoretinal surface in eyes with advanced AMD.[10]

Glial fibrillary acidic protein$^+$ processes have also been observed overlying Bruch's membrane in atrophic areas of GA eyes.[6,8,10–12] These authors did not, however, characterize these membranes nor determine their frequency or association with pathology. Müller cell extension through the ELM would affect the milieu of both the subretinal space and retina. These changes may contribute to RPE cell loss by promoting inflammation and allowing the flow of material between the retina and subretinal space. The present study investigated Müller cell membranes posterior to the ELM in human donor eyes with GA.

Materials and Methods

Tissue Collection

Aged donor eyes with no retinal disease (age-matched controls) or GA were received from the National Disease Research Interchange (Table 1). The use of tissue was approved by the institutional review board at Johns Hopkins University. All tissues were used in accordance with the Declaration of Helsinki and written informed consent was obtained from all

Table 1. Donor Eyes Used in This Study

Donor ID	Sex	Age at Death	Eye	Ocular History	Glia on Preretinal Surface	Area of RPE Atrophy, mm²	Area of Choroidal Loss, mm²	Area With Subretinal Glia, mm²	Other Medical Problems	Cause of Death
1A	Male	90	OD	GA	Blooms	32	>50	56.4		Cardiac arrest
1B	Male	90	OS	GA	Membranes	26.4	38.8	33.3		Cardiac arrest
2	Male	94	OS	GA, RPE detachment	Blooms, membranes	6.4	16.6	5.3	HC, arthritis, osteoporosis, CHF, chronic bronchitis	CHF
3A	Female	89	OD	GA	Blooms, membranes	14.7	14.4	14.3	PMH, CHF, HTN, osteoarthritis, hypothyroidism, HC, dementia, osteoporosis, asthma	myocardial Myocardial infarction
3B	Female	89	OD	GA	Present	Cryo-preserved eye	Cryo-preserved eye	Cryo-preserved eye	PMH, CHF, HTN, osteoarthritis, hypothyroidism, HC, dementia, osteoporosis, asthma	myocardial Myocardial infarction
4	Female	98	OD	GA	Present	Cryo-preserved eye	Cryo-preserved eye	Cryo-preserved eye	Colon cancer	Stroke
5	Female	98	OD	GA	Present	TEM	TEM	TEM		Abdominal cancer
6	Male	78	OD	None	None	0	0	0	HTN, Parkinsons, dementia, DM	Parkinsons
7	Female	75	OS	None	Sprouts	0	0	0	breast cancer, dementia, recurring UTI, sinus headaches, arrhythmia, CAD, HLD, NTN, valvular disease, OA, polymyalgia rumetatica, CABG, aortic valve replacement, appendectomy, cholecystectromy, hysterectromy, ooperectomy, salpingoophorectomy	UTI
8	Male	71	OD	None	None	0	0	0	Prostate and tongue cancer, radiation treatment, seasonal allergies, depression, bells palsy	Cardiac arrest
9	Male	85	OS	None	Sprouts	0	0	0	Apnea, COPD, HTN, neuropathy, heart stents	Cardiac arrest

This list includes available data regarding ocular and systemic diseases of donors. Glia (positive for GFAP and vimentin) observed on the vitreoretinal surface were classified as: "sprouts" are single cells, "blooms" are bundles, and "membranes" are a dense area with numerous of glia. Eyes from donor ID's marked with an asterisk were cryopreserved and shown in cross section. AF, atrial fibrillation; CAD, coronary artery disease; CAB, coronary artery bypass graft; CHF, congestive heart failure; COPD, chronic obstructive pulmonary diseas; DM, diabetes mellitus; GA, geographic atrophy; HC, high cholesterol; HLD, hyperlipidemia; HTN, hypertension; OD, oculus dexter; OS, oculus sinister; OU, oculus uterque; NTN, nephrotoxic serum nephritis; UTI, urinary tract infection.

Table 2. List of Antibodies and Stains Used in This Study

Antibody	Structures Labelled	Source	Location	Dilution
Ck-a-GFAP	Astrocytes & activated Müller cells	Millipore	Billerica, MA	1:500
Ck-a-vimentin	Müller cells	Millipore	Billerica, MA	1:500
Rb-a-GFAP	Astrocytes & activated Müller cells	Dako	Carpinteria, CA	1:200
Rb-a-CD34	Blood vessels	Abcam	Cambridge, MA	1:200
Ms-a-GS	Müller cells	Millipore	Billerica, MA	1:500
Rat-a-CD44	Müller cell apical processes at the ELM	R&D	Minneapolis, MN	1:200
FITC conjugated PNA	Photoreceptor inner & outer segments	Vector Laboratory	Burlingame, CA	1:500
Gt-a-Rb Alexa Fluor 647		Molecular Probes/ThermoFisher	Waltham, MA	1:300 (flatmount) 1:500 (sections)
Gt-a-Ck cy3		Jackson Immunoresearch	West Grove, PA	1:300 (flatmount) 1:500 (sections)
DAPI	Nuclei	Invitrogen	Carlsbad, CA	1:1000
Gt-a-Ms cy3		Jackson Immunoresearch	West Grove, PA	1:300 (flatmount) 1:500 (sections)
Gt-a-Ms Alexa Fluor 647		Molecular Probes/ThermoFisher	Waltham, MA	1:300 (flatmount) 1:500 (sections)
UEA lectin	Endothelial Cells	Genetex	Irvine, CA	1:100

participants. Enucleated eyes were shipped on wet ice overnight to achieve post mortem times of less than 24 hours. Eyes were processed as previously described.[10]

Cryopreservation, Histology, and Immunohistochemistry

Whole eye cups were cryopreserved with a sucrose gradient as previously described.[13] Eight-micron sections were cut on a Leica cryostat (Leica Biosystems, Buffalo Grove, IL, USA). Cryosections, taken from the macula but not including the Henle fiber layer, were processed for immunohistochemistry as previously described.[14] Eyes for transmission electron microscopy (TEM) were fixed in 2.5% gluteraldehyde/2% paraformaldehyde (PFA) in 0.1 M cocadylate buffer and processed as previously reported.[13] Hematoxylin and eosin staining was performed using standard methods.

The posterior poles from wholemount retinas were immunohistochemically stained as previously described.[10] The choroids were stained with Ulex Europaeus Agglutinin (UEA)-lectin and antibodies as previously described.[15] Only UEA-lectin results are reported herein for choroids. Antibody details are listed in Table 2.

Imaging and Analysis

All images were collected on a Zeiss 710 confocal microscope equipped with Zen software (Carl Zeiss, Peabody, MA, USA). Retinas were imaged with both the ILM and the ELM en face. Maps (9 × 9 mm) were generated of the posterior poles and submacular choroids by taking tiled Z stacks at low magnification (5×). These images were collected at 1024 × 1024 resolution. High-resolution images (2048 × 2048) were collected at 20× with the optimal slice settings.

Calculation of Area Using ImageJ

The affected area was calculated from tiled images of the entire posterior pole or submacular choroid as well as gross images using ImageJ software (http://imagej.nih.gov/ij/; provided in the public domain by the National Institutes of Health, Bethesda, MD, USA). Images were opened in ImageJ and calibrated using the embedded scale bar. The free selection tool was used to draw the affected region and the area was measured. The area of RPE atrophy was defined as the area where choroidal vessels are visible in the gross photos. A similar method is used by clinicians to monitor GA progression using fundus photographs.[16] For each eye, the area of RPE atrophy, choroidal vessels (CC) loss, and subretinal glia were entered into Microsoft Excel (Redmond, WA, USA). The correlation coefficient was calculated using Microsoft Excel.

Results

Normal Aged Retina

Aged retinas with no pathology were used as controls in this study. The gross image of a representative control retina demonstrated the normal retinal arcade vessels, optic disc, and fovea (Fig. 1A). Choroidal vessels, blocked by an intact RPE monolayer, were not visible. Ulex Europaeus Agglutinin–lectin staining of isolated choroid revealed a uniform pattern of choriocapillaris throughout the submacular choroid (Fig. 1B). The retina imaged with the ILM en face demonstrated a uniform staining of GFAP$^+$ astrocytes and vimentin$^+$ Müller cell endfeet (Fig. 1C). Higher magnification better demonstrated the Müller cell endfeet and revealed isolated GFAP$^+$/vimentin$^+$ glial cells on the vitreoretinal surface (Fig. 1D). Vimentin and GFAP staining were barely detectable when viewed with the ELM en face at low magnification as a tiled map (Fig. 1E). The honeycomb-like pattern created by the vimentin$^+$ Müller cell processes as they form the ELM was visible at higher magnification (Fig. 1F). No vimentin or GFAP$^+$ processes were observed posterior to the ELM in aged control retinas.

Glia on the Vitreoretinal Surface in GA Eyes

Imaging of retinas with GA with the ILM en face revealed glial cells and processes positive for GFAP and vimentin on the vitreoretinal surface (Fig. 2). There was no correlation between GA severity and the amount of preretinal glia. For example, a retina (from the eye shown in Figs. 3D–F) with a small atrophic area had a large glial membrane, which covered most of the posterior pole (Figs. 2A–F). The retina shown in Figures 3G to 3I with a large atrophic area had many glial processes and cells on the vitreoretinal surface but no membrane (Figs. 2G–L).

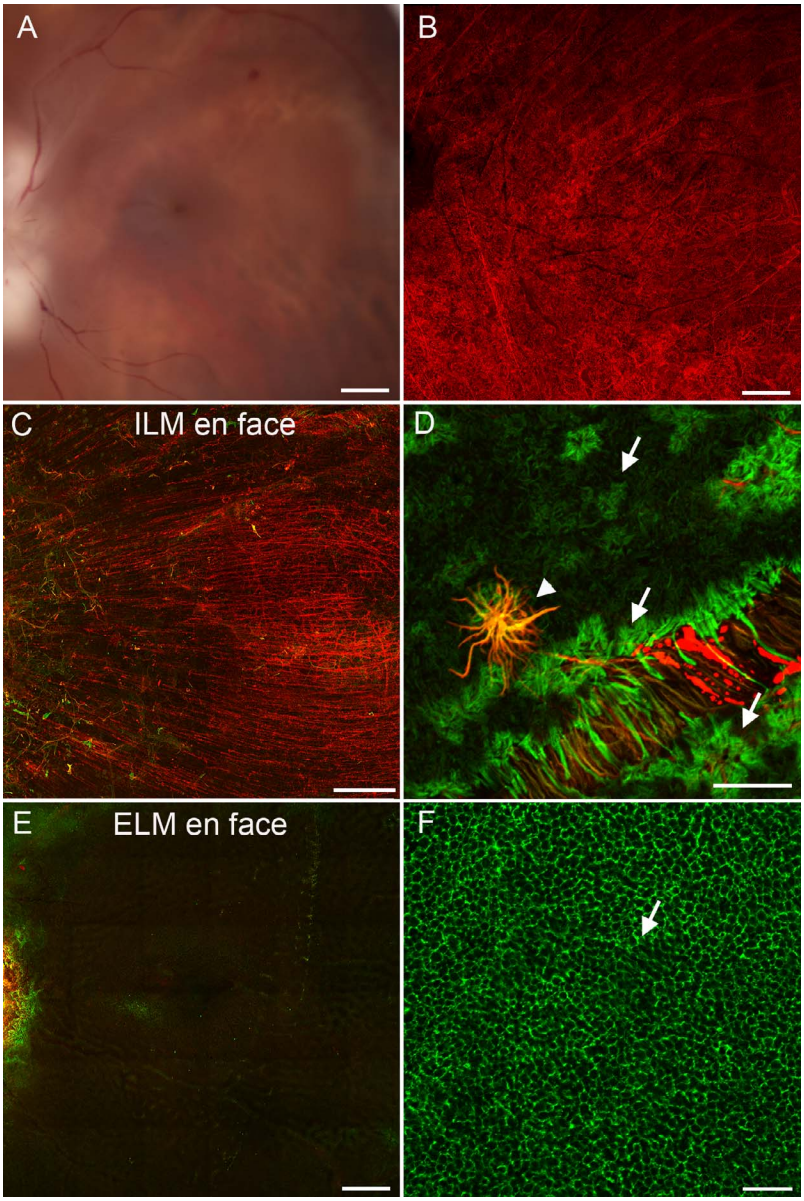

Figure 1. A representative 75-year-old age-matched control retina. (**A**) Gross fundus photograph of the posterior pole from Donor 7 in which the choroid is blocked by RPE cells. (**B**) The control choroid stained with UEA-lectin demonstrated the density of submacular choriocapillaris. (**C**, **D**) The retinal posterior pole stained for GFAP (*red*) and vimentin (*green*) and imaged with the ILM en face demonstrated a uniform astrocyte pattern with only a few isolated vimentin$^+$ and GFAP$^+$ glia on the vitreoretinal surface. (**D**) At higher magnification, the vimentin$^+$ Müller cell endfeet (*arrows*) and GFAP$^+$ astrocyte processes ensheathing a vessel were observed with an isolated double-positive glial cell on the vitreoretinal surface (*arrowhead*). Note that ripples in the tissue forced some endfeet to be out of focus. (**E**, **F**) This same retina imaged with the ELM en face. At low magnification, staining was barely visible. (**F**) Higher magnification revealed the cobblestone pattern created by vimentin$^+$ Müller cell apical processes (*arrow*). *Scale bars*: (**A**, **B**, **E**) 1 mm; (**C**) 500 μm; (**D**, **F**) 50 μm.

Glia Extended Beyond the ELM in All GA Eyes

In all eyes with GA, gross images revealed atrophic areas where RPE cell loss made large choroidal vessels visible (Figs. 3A, 3D, 3G, 3J). Drusen, seen as small white spots, were also observed surrounding the atrophic area (Figs. 3G, 3J). Ulex Europaeus Agglutinin–lectin staining of the submacular choroid revealed choriocapillaris dropout corresponding to areas of RPE atrophy (Figs. 3C, 3F, 3I). A clear border was evident in all atrophic areas. When retinas stained for GFAP and vimentin were imaged with the ELM en face, a glial membrane was observed covering an area very similar to that of RPE and choriocapillaris atrophy (Figs. 3B, 3E, 3H, 3K). As shown in Figure 3, subretinal glial membranes were observed in all GA eyes investigated. The subretinal glial membranes were all similar in shape and size to the atrophic areas. Subretinal membranes ranged in area from 5.3 to 56.4 mm^2 (Table 1). Similarly, the area of RPE atrophy, measured from gross photos as the area where large choroidal vessels were visible, ranged from 6.4 to 32 mm^2 while choriocapillaris loss ranged from 14.4 to greater than 50 mm^2. It is important to note the gross photos were taken of concave eyecups while the retina and choroid images were collected on flat tissue. There was significant correlation between the area of the subretinal glial membrane and both RPE atrophy and CC dropout in each eye with GA (Supplementary Fig. S1).

Investigative Ophthalmology & Visual Science

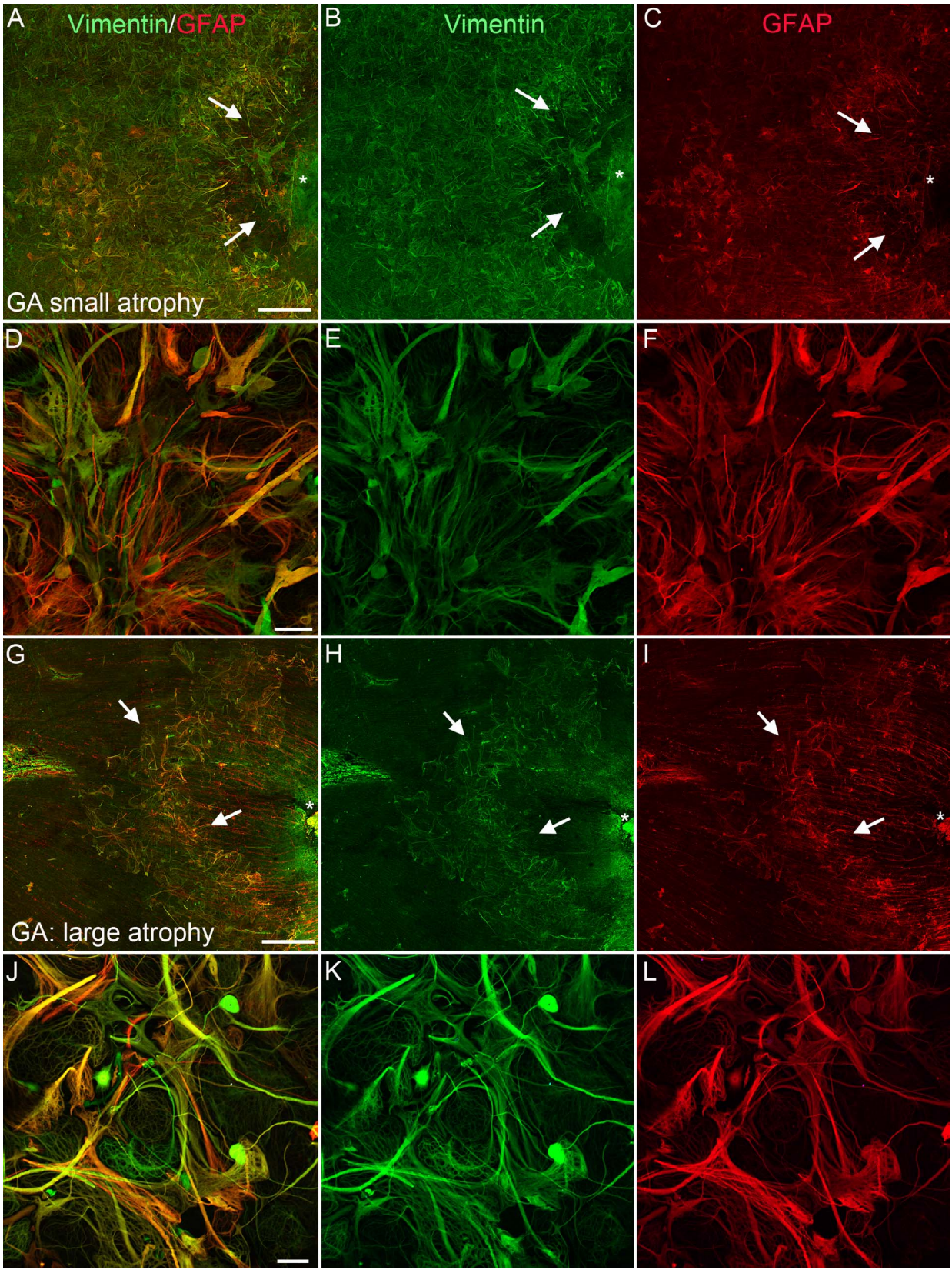

Figure 2. Retinas of subjects with GA had varied degrees of glia on the vitreoretinal surface. Wholemount retinas stained for GFAP (*red*) and vimentin (*green*) imaged with the ILM en face. (**A–F**) Low magnification image of the retina from Donor 2, with a small atrophic area, taken between the fovea (*asterisk*) and optic disc (not shown) revealed a large glial membrane, which covered most of the posterior pole. Only the parafoveal region (*arrows*) was spared from this membrane. The entire area to the *left* of the *arrows* was covered by a preretinal membrane. (**D–F**) Higher magnification of this membrane confirmed that cells are double-positive for GFAP and vimentin. The density of the membrane was also demonstrated. (**G–I**) Low-magnification image of the retina from Donor 1, with a large atrophic area, taken between the fovea (*asterisk*) and optic disc (not shown) demonstrated glial blooms on the vitreoretinal surface (*arrows*). (**J–L**) Higher magnification revealed the density of this bloom, which contained numerous cells and processes. *Scale bars*: (**A–C**), (**G–I**) 1 mm; (**D–F**), (**J–L**) 50 μm.

Investigative Ophthalmology & Visual Science

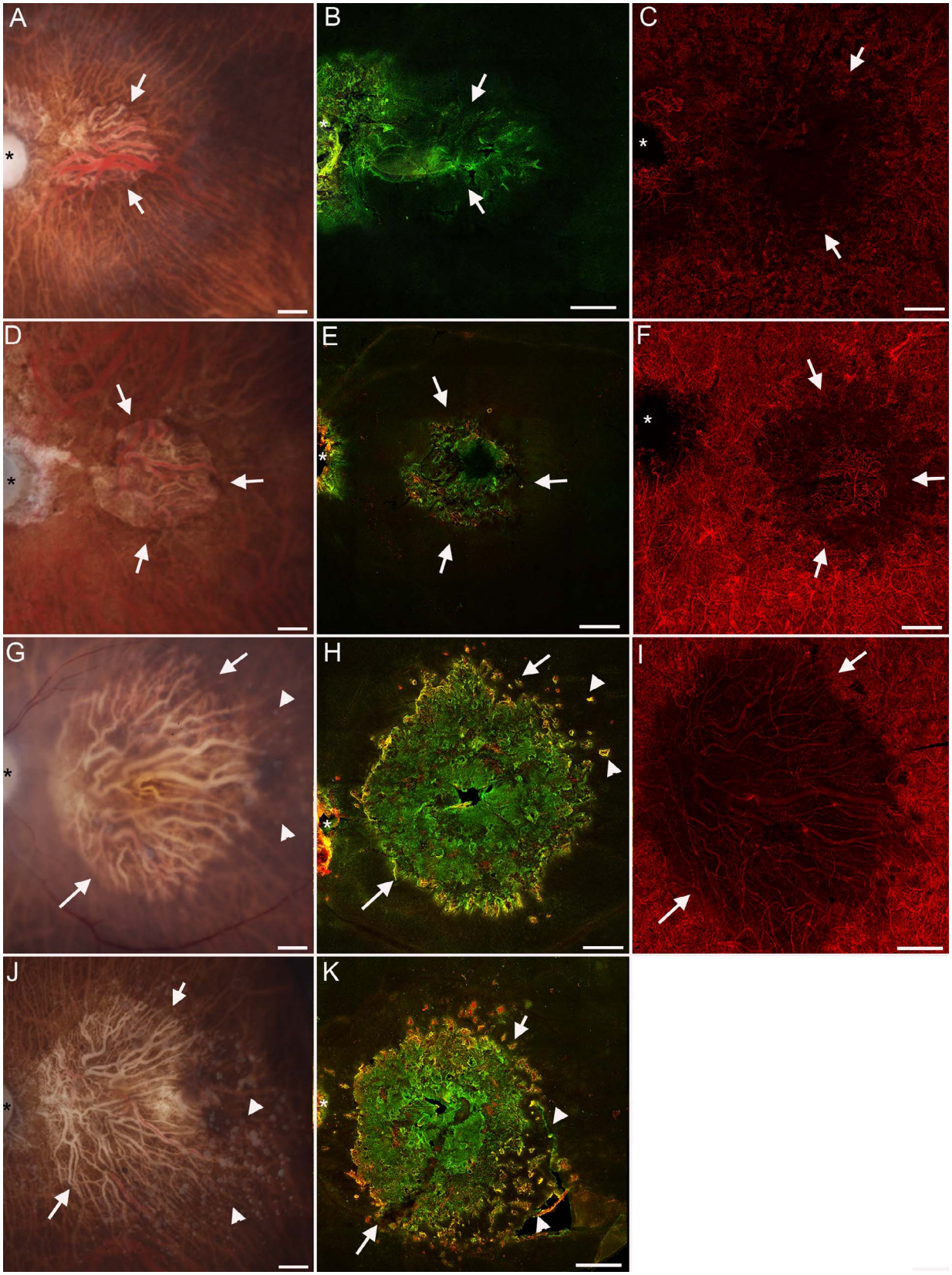

Figure 3. Glia created a membrane posterior to the ELM in atrophic areas of GA eyes. Gross fundus photographs (**A**, **D**, **G**, **J**) of eyes from donors with GA (Donors 3A, 2, 1A, and 1B, respectively) showing varied areas of RPE atrophy. The loss of RPE (*arrows*) allowed the choroidal vessels to be visible. *Arrowheads* point to drusen in (**D**) and (**G**). (**B**, **E**, **H**, **K**) Retinas stained for GFAP (*red*) and vimentin (*green*) were imaged with the ELM en face revealing glial membranes (*arrows*), which closely matched the atrophic area. *Arrowheads* point to small glial projections through the ELM in (**H**) and (**K**). As shown, most processes were positive for both GFAP and vimentin. (**C**, **F**, **I**) Choroidal vessels stained with UEA lectin (*red*) were attenuated posterior to the atrophic RPE region (*arrows*). *Scale bars*: 1 mm. *Asterisks* indicate the optic nerve. The choroid of the retina shown in (**J**) and (**K**) (from Donor 1B) was processed differently and, therefore, could not be included in this figure.

Investigative Ophthalmology & Visual Science

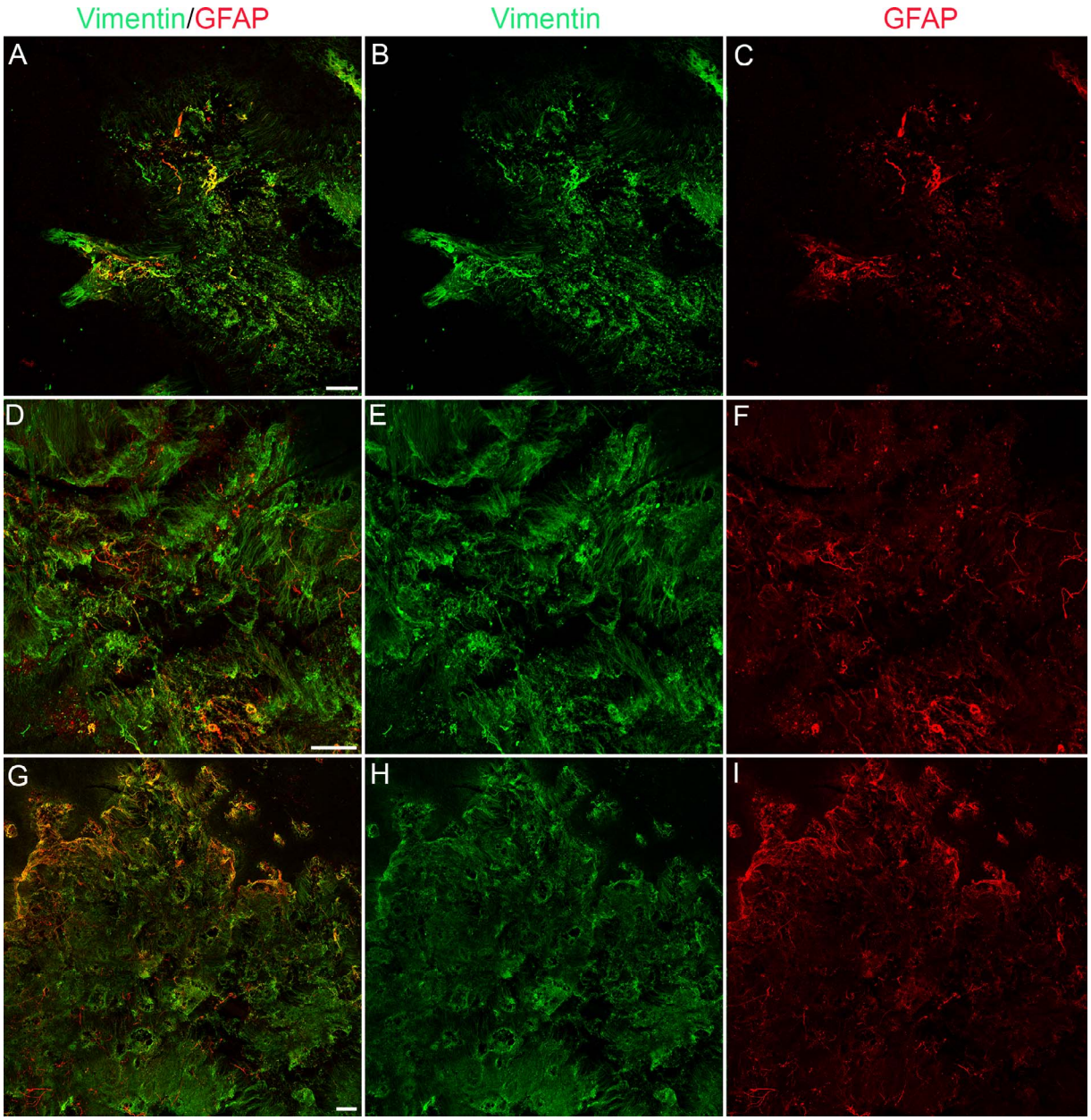

Figure 4. Glial membranes increase in density with increased area of atrophy. Retinas from Figure 3 stained with GFAP and vimentin imaged with the ELM en face shown here at higher magnification. (**A–C**) In a retina with the smallest atrophic area (Donor 3A), only a few GFAP$^+$ processes were observed among many vimentin$^+$ processes. (**D–F**) The glial membrane in a retina with a slightly larger atrophic area (Donor 2) was larger and denser than that shown in (**A–C**) and had more GFAP$^+$ processes. (**G–I**) The membrane from Donor 1A, the retina with the largest atrophic area, contained numerous processes that were positive for both vimentin and GFAP. *Scale bars*: (**A–C**) 100 µm; (**D–I**) 200 µm.

While some processes within this membrane were double positive for GFAP and vimentin, more were only vimentin$^+$. A few cell processes had GFAP but not vimentin. Adjacent to this large membrane, small bundles of GFAP/vimentin double-positive cells were observed projecting into the subretinal space. The depth of these structures was demonstrated more clearly when viewing membranes at higher magnification (Figs. 4, 5). Labeling with vimentin was dominant, but most processes also had GFAP. Glial fibrillary acidic protein was more prominent in the larger membrane (Figs. 4G–I). Thin processes were observed in a focal plane posterior to the ELM (Fig. 5A). These processes were disorganized and skewed. In many areas, processes overlapped one another. In other areas, they joined to create bundles in the subretinal space. These bundles were most apparent at the membrane's edge. Some processes joined and terminated in circular formations, which surrounded process-free areas. Glial fibrillary acidic protein$^+$/vimentin$^-$ processes were more linear and less complex than those that were double positive or expressed only vimentin. At the ELM focal plane, Müller cell processes within the membrane extended horizontally across the retinal surface (Fig. 5B). While the ELM's honeycomb-like pattern was lost within the membrane, connections between Müller cell processes were observed. These Müller cell connections were more prominent away from the membrane's center and resembled the ELM near the edge (Fig. 5B). Large gaps

Investigative Ophthalmology & Visual Science

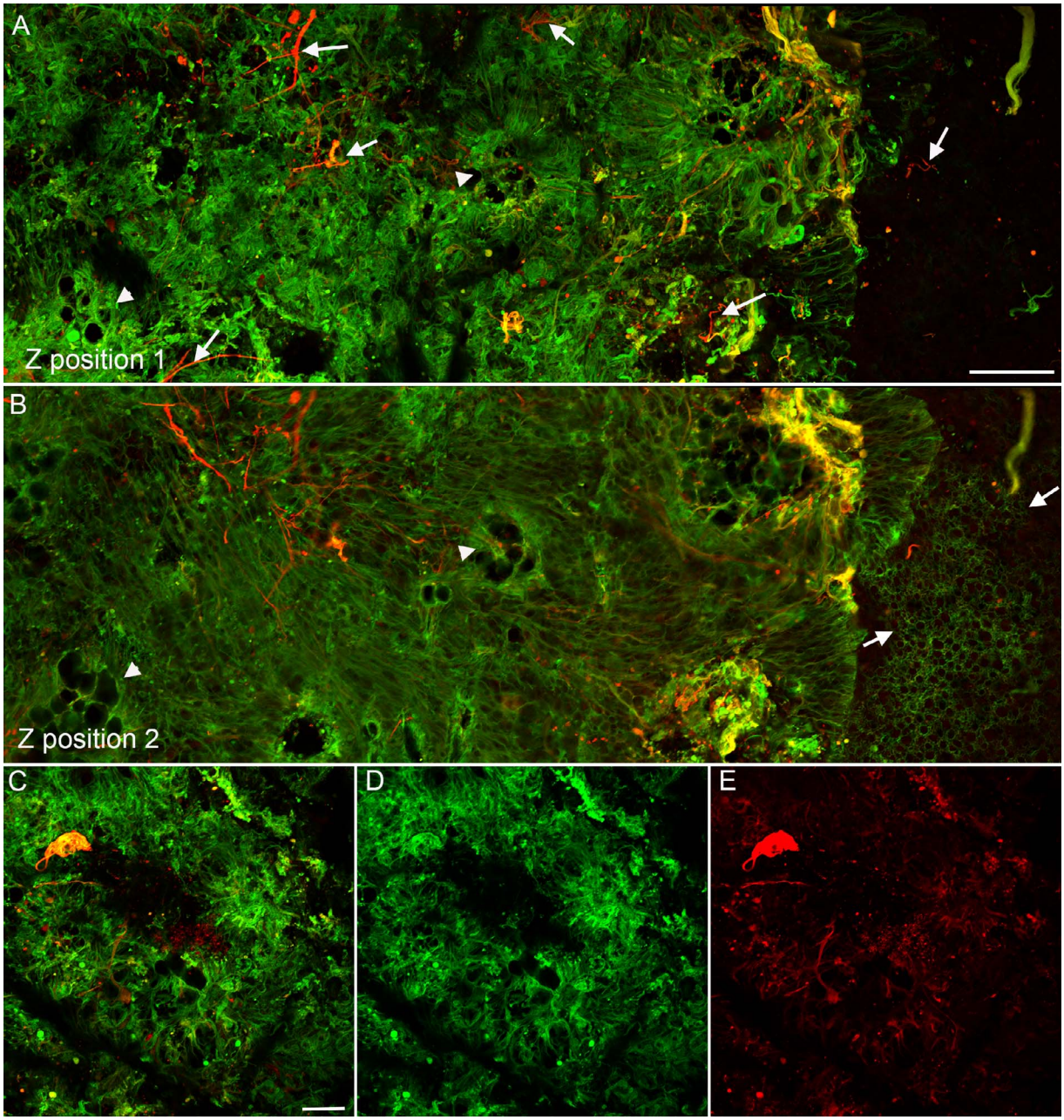

Figure 5. Glial membranes had a defined border. A retina from Donor 1 with GA stained for GFAP (*red*) and vimentin (*green*). (**A**) At the focal plane posterior to the ELM (Z-position 1), linear processes of Müller cells could be seen extending along the bottom of the retina to create a dense membrane. Many of these same processes had GFAP as well as vimentin (*yellow labeling*). A few had only GFAP (*arrows*). A clear border was observed to this membrane. At the membrane's edge, cells were intensely positive for GFAP. The membrane contained frequent gaps with no glial processes (*arrowhead*). (**B**) At the focal plane of the ELM (Z position 2), the normal cobblestone pattern was observed just beyond the membrane (*arrow*). Müller cell processes at this plane had elongated, often overlapping processes and juxtapositions between individual processes can be observed. Müller cell processes appeared condensed around the holes observed in the first focal plane (*arrowhead*). (**C–E**) In the center of the atrophic area, in the Z plane posterior to the ELM, connections between glial processes were clearly observed. Processes with only GFAP were observed among those with vimentin and GFAP. *Scale bars*: (**A**, **B**) 100 μm; (**C–F**) 50 μm.

between vimentin$^+$ cells were also evident in areas corresponding to the circular structures in the posterior focal plane. Individual processes positive for only GFAP appeared bulbous and were observed throughout the membrane (Fig. 5B). The membrane contained a clear border beyond which the cobblestone pattern of the ELM was evident. In the center of this gliotic lesion, some GFAP$^+$ processes were observed among those that were double positive and these processes were the most disorganized (Figs. 5C–E).

The smaller glial projections adjacent to the atrophic area were also evaluated at higher magnification (Fig. 6). Thick glial processes, positive for GFAP and vimentin, encircled one another and created nodule-like structures external to the ELM (Figs. 6A–C). In the next focal plane, finer vimentin$^+$/GFAP$^-$ processes were evident inside the band of thick double-positive processes (Figs. 6D–F). At the ELM focal plane, a small break was evident anterior to this lesion (Figs. 6G–I). Vimentin$^+$ processes extending from the retina

Investigative Ophthalmology & Visual Science

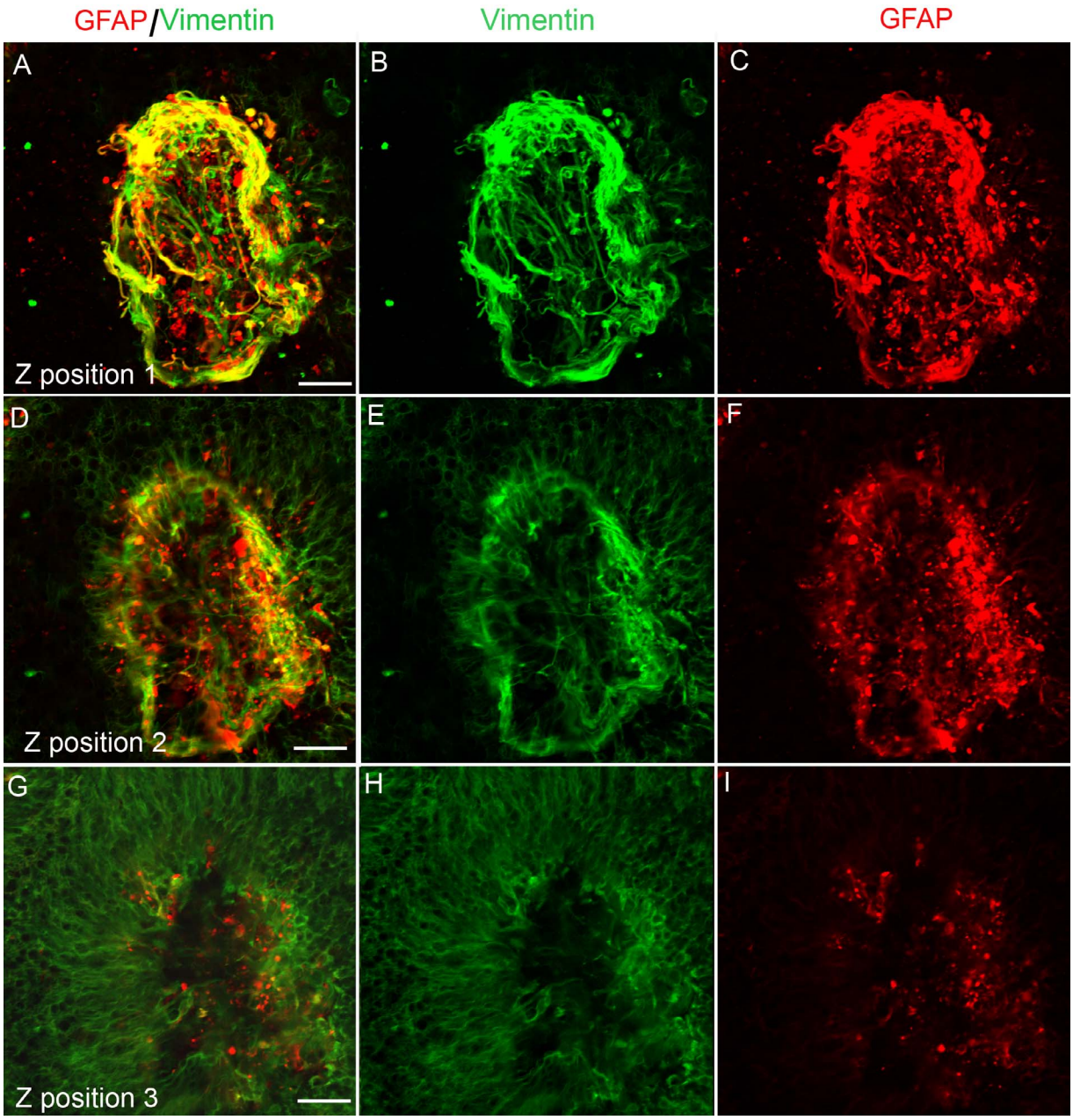

Figure 6. Nodules of glia and breaks in the ELM were observed adjacent to the membrane. The same retina shown in Figures 3 and 4 from Donor 1 with GA stained for GFAP (*red*) and vimentin (*green*) was imaged with the ELM en face. The small projections indicated by the *arrowheads* in Figure 3H are shown here at higher magnification. (**A–C**) Glial cells were observed extending into the subretinal space and encircling their exit point at the focal plane posterior to the ELM (Z position 1). Glial fibrillary acidic protein was most intense at the border and was punctate within the nodule while vimentin intensely stained Müller cell processes. (**D–F**) Closer to the ELM focal plane (Z position 2), disorganized Müller cell processes extended through a break in the ELM. The thick band of vimentin$^+$/GFAP$^+$ processes was still present surrounding the exiting cells. Glial fibrillary acidic protein staining (**F**) was more punctate at this focal plane. (**G–I**) At the level of the ELM (Z position 3), a break in the ELM was clearly evident. Müller cells adjacent to this break extended horizontally away from the break before a normal ELM pattern was observed. Glial fibrillary acidic protein was limited to a few punctate areas. The ELM had only very weak GFAP staining. *Scale bars*: 20 µm.

replaced the normal ELM in this area. Glial fibrillary acidic protein staining was very bulbous within this small lesion closer to the ELM but was observed in subretinal cell processes.

Cross sections taken from cryopreserved eyes with GA were labeled with vimentin, GFAP, and peanut agglutin (PNA) to verify that the gliotic lesions coincided with RPE and photoreceptor loss. In the nonatrophic region, where PNA$^+$ photoreceptor segments were visible, vimentin labeled the entire Müller cell length (Figs. 7A, 7B). Müller cell apical processes and photoreceptor inner segments created a clearly defined ELM. Glial fibrillary acidic protein was primarily confined to astrocytes in the nonatrophic area (Figs. 7A, 7C). At the border of the atrophic area, photoreceptors appeared to have lost their polarity and segments extended horizontally instead of vertically (Figs. 7A, 7B, 7D, 7E). Müller cell processes in this area were GFAP$^+$ and had a more horizontal orientation (Figs. 7A–C,

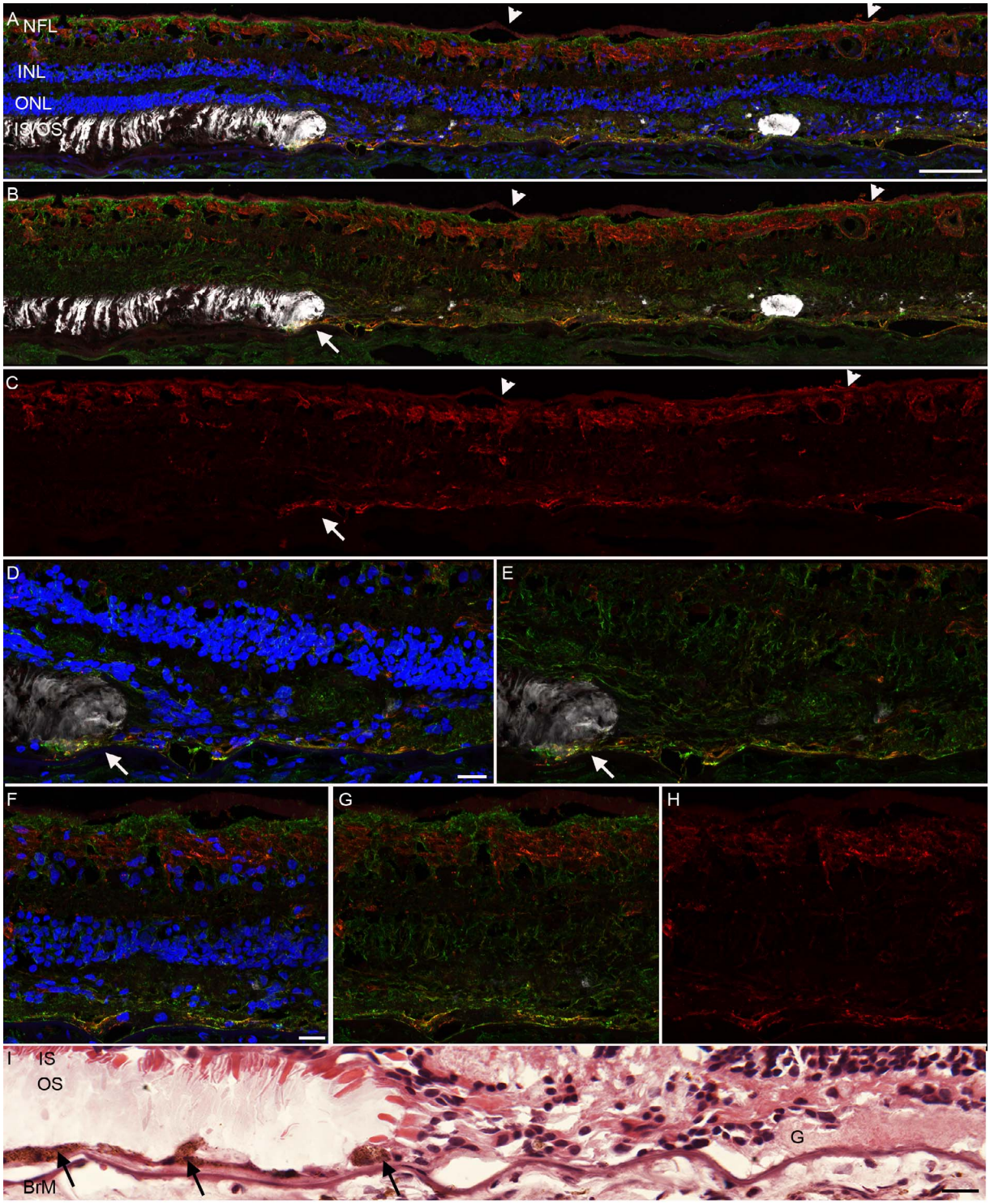

Figure 7. Sections confirmed that vimentin^{+}/GFAP^{+} membrane was posterior to areas of photoreceptor atrophy. Cross sections from the eye of Donor 4 with GA were stained for vimentin (*green*), GFAP (*red*), PNA (*white*), and 4′,6-diamidino-2-phenylindole (DAPI) (*blue*). (**A–C**) In the nonatrophic area, evident by PNA-labeled photoreceptor segments and a near complete ONL, GFAP was confined to the astrocytes within the nerve fiber layer while vimentin revealed the linear morphology of Müller cells. At the border of atrophy, the photoreceptor segments appeared bundled and Müller cell processes, lightly positive for GFAP, were less linear. A GFAP^{+}/vimentin^{+} membrane (*arrow*) was observed posterior to the bundled segments. This membrane occupied the remnant subretinal space and ONL in the atrophic area. Glia were also observed on the vitreoretinal surface (*arrowhead*). (**D–E**) Higher magnification of the border demonstrated glia below the PNA bundles (*arrow*) as well as the disorganized appearance of GFAP^{+}/vimentin^{+} Müller cells within the membrane. Numerous nuceli within the membrane appeared to be part of Müller cells. (**F–H**) In the atrophic area, GFAP^{+}/vimentin^{+} processes were still disorganized and occupied the remnant ONL. Some nuclei were observed that were GFAP^{+}/vimentin^{-}. (**I**) Hematoxylin and eosin staining of an adjacent section clearly demonstrated the glial processes abut Bruch's membrane. *Arrows* indicate pigmented RPE cells adjacent to the atrophic area. No pigmented cells were noted in the membrane. BrM, Bruch's membrane; G, glia; IS/OS, inner segments and outer segments. *Scale bars*: (**A–C**) 100 μm, (**D–H**) 20 μm, (**I**) 20 μm.

Investigative Ophthalmology & Visual Science

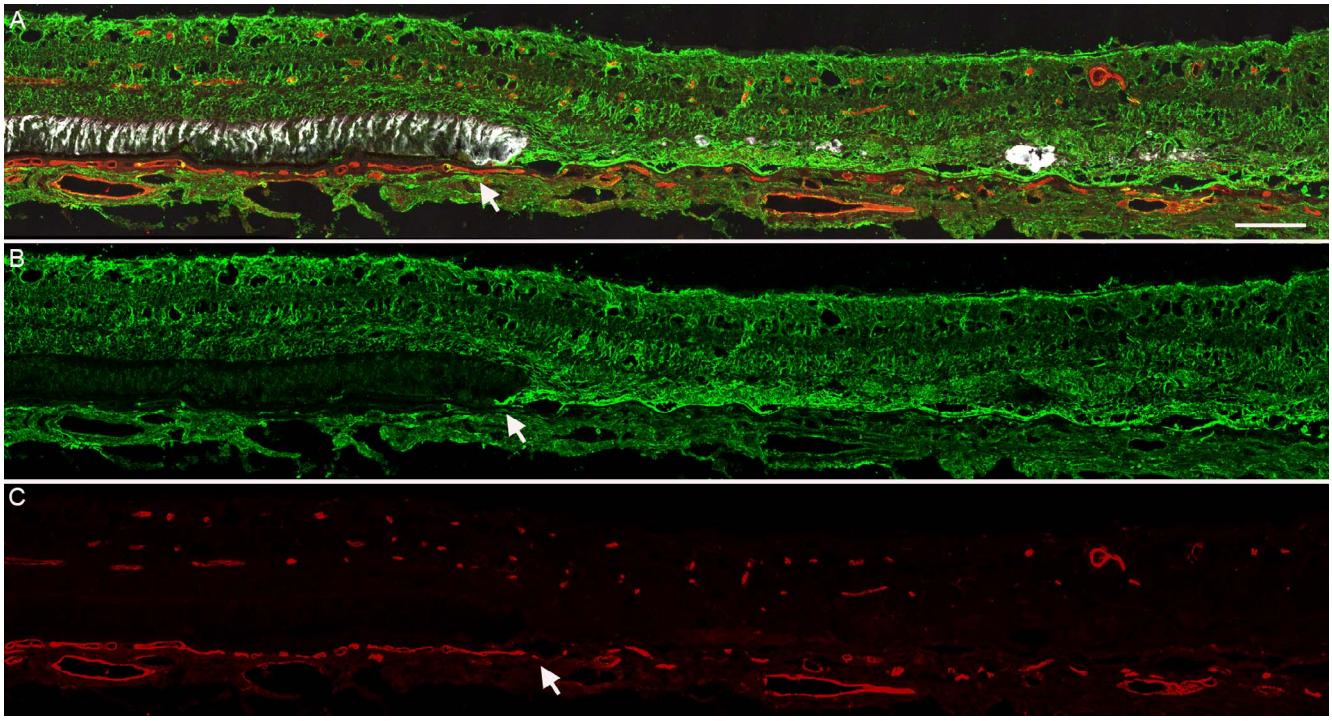

Figure 8. Sections confirmed that vimentin$^+$ membrane was anterior to an area with choriocapillaris dropout. (**A–C**) A cross section from the eye of Donor 4, adjacent to those used in Figure 7, were stained for vimentin (*green*), CD34 (*red*; blood vessels), and PNA (*white*). In the nonatrophic area, PNA$^+$ outer segments and linear vimentin$^+$ Müller cell processes were observed anterior to a continuous CD34$^+$ choriocapillaris. In the atrophic area, however, a vimentin$^+$ membrane occupies the subretinal space posterior to the few remnant PNA$^+$ segments. Choriocapillaris was greatly reduced (**C**). *Arrows* indicate the border of atrophy where choriocapillaris vessels return to normal and the glial membrane ends as PNA$^+$ segments return to normal.

7D, 7E). A thick band of GFAP$^+$/vimentin$^+$ glial processes with some DAPI$^+$ nuclei were observed posterior to these segments. This band ended abruptly where photoreceptor segments regain their linear morphology. In the atrophic area, GFAP$^+$/vimentin$^+$ processes occupy the remnant subretinal space in place of photoreceptor segments (Figs. 7A–H). Müller cell processes within the retina anterior to this atrophic area were GFAP$^+$ and disorganized. While a few DAPI$^+$ nuclei were observed in the ONL anterior to the glial membrane, these appeared to be vimentin$^+$ cells. DAPI staining was also observed within the glial membrane. Focal areas with PNA labeling were observed anterior to the membrane. Müller cells anterior to the membrane were not as linear and appeared disorganized compared with the nonatrophic area. The subretinal location of the membrane was confirmed by staining an adjacent section with hematoxylin and eosin (Fig. 7I). Retinal pigment epithelial cells are observed adjacent to the atrophy but no pigmented cells were observed within the subretinal membrane. This image also demonstrated that glia abut Bruch's membrane and, in one area, appeared to merge with Bruch's membrane. An adjacent section was stained for vimentin, CD34 (blood vessel marker), and PNA (Fig. 8). As suggested by flatmount analysis, choriocapillaris loss was observed in the atrophic area and coincided with the subretinal vimentin$^+$ membrane.

Cryosections from a donor with GA stained for vimentin and GS confirmed the linear morphology of Müller cells in the nonatrophic area (Figs. 9A–E). Peanut agglutin staining demonstrated the atrophic border. In the atrophic area, GS appeared to be reduced within the retina but was present within the subretinal glial membrane (Figs. 9F, 9G).

ELM Disruption was Evident in Atrophic Areas of GA Eyes

In the nonatrophic area, staining with anti-CD44, which labels Müller cell apical processes, demonstrated an intense, continuous band at the ELM (Figs. 10A–C). In addition, astrocytes and Müller cell processes within retina were lightly CD44$^+$. CD44 expression was drastically altered in the atrophic area, particularly at the ELM (Figs. 10D–I). The band of staining at the ELM was replaced by punctate CD44 staining observed at both the level of the ELM and at the edge of processes extending into the remnant subretinal space. The CD44$^+$ ELM adjacent to glial membranes supports the subretinal location of membranes (Figs. 10D–F). The rapid disruption of the ELM also indicates the clear border observed in wholemounts. CD44 was also observed in the glial cells on the vitreoretinal surface (Figs. 10A, 10C, 10D, 10F).

TEM Confirms Glia in the Subretinal Space of GA Eyes

Transmission electron microscopy analysis was used to further verify that glial cells were posterior to the ELM. Müller cell processes were observed adjacent to Bruch's membrane in areas missing photoreceptors and RPE cells (Fig. 11). In some areas, Müller cell processes were observed within Bruch's membrane and adjacent to choriocapillaris. As noted above, no pigmented cells were observed within the membrane.

Discussion

Glial cells, positive for vimentin and/or GFAP, extended beyond the ELM and created dense gliotic membranes in areas of RPE

Investigative Ophthalmology & Visual Science

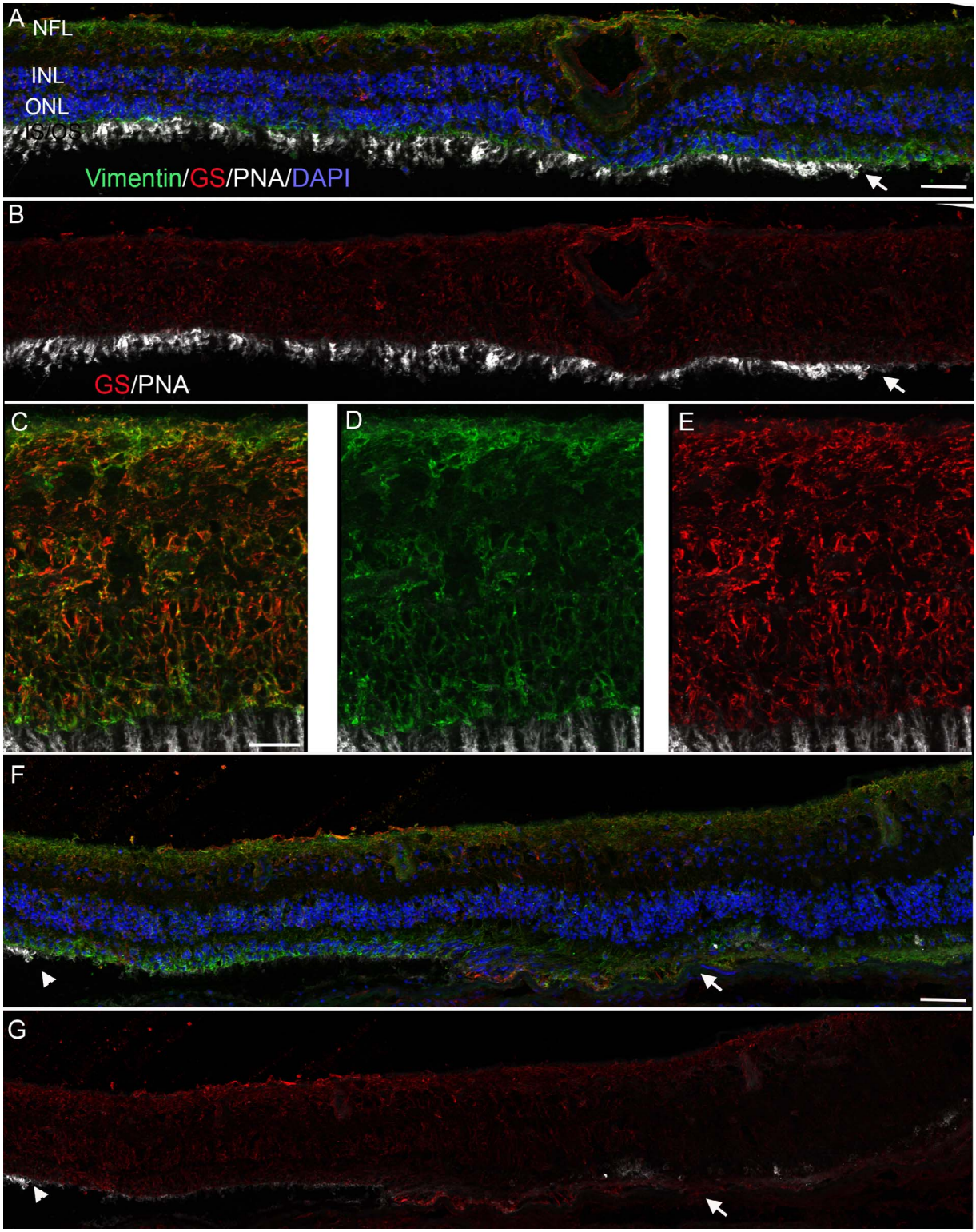

Figure 9. Müller cells within subretinal membranes expressed glutamine synthetase. Cross sections taken from the eye of Donor 3 with GA were stained for vimentin (*green*), GS (*red*), PNA (*white*), and DAPI (*blue*). (**A**, **B**) In the nonatrophic area, both vimentin and GS were observed the entire width of Müller cells. Peanut agglutin–labeled segments were reduced in length closer to the atrophic area and end at the atrophic border (*arrow*). (**D**, **E**) Higher magnification of the non-atrophic area better demonstrates the linear morphology of Müller cells. (**F**, **G**) In the atrophic region, as evidenced by only PNA-stained remnants (*arrowhead*) and a largely absent ONL, GS staining appears to be reduced. Some staining was observed within the glial membrane, which colabeled with that of vimentin (*arrow*). *Scale bars*: 50 μm.

Investigative Ophthalmology & Visual Science

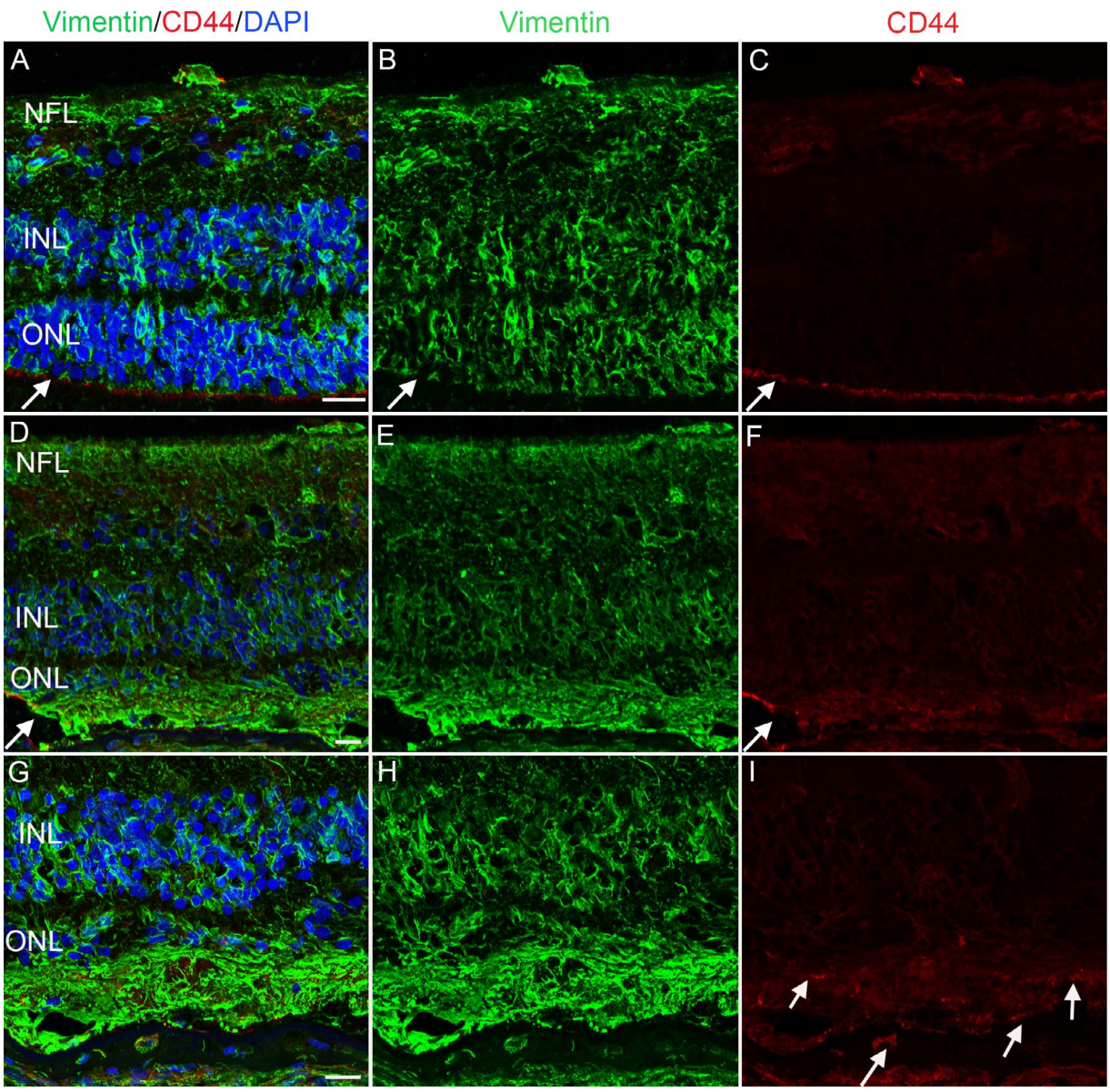

Figure 10. CD44 in the ELM was disrupted in atrophic areas. The posterior pole of an eye with GA (Donor 3) was stained for vimentin (*green*) and CD44 (*red*). (**A–C**) In a nonatrophic area, CD44 was most prominent in the Müller cell microvilli, creating a line at the ELM. CD44 was also detected within astrocytes within the nerve fiber layer. (**D–F**) CD44 labeling (*arrow*) dropped off abruptly as the glial membrane forms. Within the glial membrane, CD44 was punctate and expression by Müller cells within the retina was more intense than in the nonatrophic region. Vimentin$^+$ Müller cells were not as linear as those within the nonatrophic area and create a dense membrane. (**G–I**) A higher magnification of the glial membrane further demonstrates its thickness and the punctate CD44 staining in this area. Müller cells within the membrane were disorganized. *Scale bars*: 20 μm.

and photoreceptor atrophy in eyes with GA. These membranes were present in all GA eyes investigated and were confined to the atrophic area. The ELM of GA eyes had a normal cobblestone appearance surrounding the atrophic area. No subretinal glia were observed in the posterior pole of normal aged retinas.

Glial membranes in all GA retinas had succinct borders that were almost identical to those of RPE loss and choriocapillaris dropout. Similar glial membranes, often termed "seals," have been reported in human and rodent retinas with retinitis pigmentosa as well as retinal detachment.[17–19,20–24] Müller cell processes also extend through the ELM following laser injury in rats.[25] It has been suggested that Müller cells respond to photoreceptor death by proliferating to fill in gaps left by dying cells. Müller cell–Müller cell junctions may replace Müller cell–photoreceptor junctions in these cases.[21] It seems plausible to hypothesize, therefore, that Müller cells in eyes with GA created a membrane in response to losing their ELM binding partner, photoreceptors. A recent study, however, observed that Müller cells only occupied the subretinal space in one of four mouse models with photoreceptor loss.[21] Therefore, photoreceptor loss alone is not enough to disrupt the ELM and other factors, perhaps from RPE, must stimulate Müller cell migration out of retina.

Glial "seals" as reported in retinitis pigmentosa eyes as well as animal models of retinal detachment and degeneration

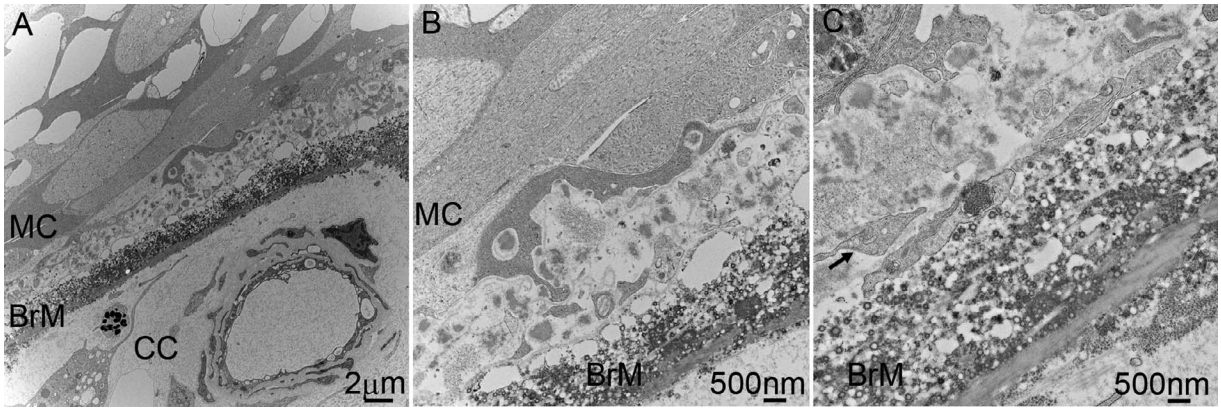

Figure 11. Transition electron microscopy confirms subretinal localization of glia. An eye with GA (Donor 5) was analyzed with TEM. (**A**) Müller cell processes (MC) were adjacent to Bruch's membrane (BrM) where the RPE cells are missing. (**A**) Müller cell processes (MC) were adjacent to BrM where the RPE cells are missing. Choroidal vessels (CC) were observed below. (**B**) A closer look at Müller cells above BrM. (**C**) Müller cell processes (*arrows*) were also observed within BrM. *Scale bars*: (**A**) 2 μm, (**B**, **C**) 500 nm.

appear to be layers of overlapped Müller cell processes.[20–22,26,27] It seems plausible that a similar, single-layered glial seal would also form in the atrophic area of GA eyes if photoreceptor loss was the primary stimulant for Müller cell process migration. The glial membranes reported herein, however, are dense, multilayered structures. DAPI$^+$/vimentin$^+$ glia within the subretinal space and the remnants of ONL suggest that some Müller cell bodies are migrating and/or proliferating rather than simply extending processes. Moreover, focal PNA staining was observed anterior to glial membranes in the present study, indicating that membranes are present even in areas with surviving photoreceptors. The remnant PNA staining is reminiscent of outer retinal tubulations that have been reported in GA eyes.[28,29] These observations suggest that additional stimuli must contribute to the dense glial membranes formed in atrophic areas.

The smaller glial nodules observed beyond the ELM adjacent to the larger atrophic region (Fig. 6) may provide clues to other stimuli. In some cases, these nodules appeared to correspond with drusen observed on gross photographs. As many drusen were removed during EDTA treatment, the association between subretinal glia and drusen could not be confirmed. Drusen accumulation in eyes with GA could provide additional stimulation for Müller cell and astrocyte migration. This hypothesis is supported by a recent observation of multiple, small glial projections that corresponded to hard drusen (which remained attached to choroid) in an eye with intermediate AMD (Edwards MM, unpublished data). Glial projections beyond the ELM in areas of drusen have also been previously reported.[30] Glial fibrillary acidic protein$^+$ glial cells have also been observed accumulating in the ONL above drusen.[8] Perhaps this accumulation occurs before glia extend processes into the subretinal space.

The photoreceptor outer segments normally separate Müller cells and RPE cells. As photoreceptors die, however, these cells can interact with each other. The RPE, particularly if stressed or dying, may produce growth factors, such as TNF-α, TGF-β, and VEGF, stimulating the migration of glia into the subretinal space. Retinal pigment epithelial cells may also stimulate the proliferation and migration of Müller cells, increasing the density of glial membranes. Studies are underway in our laboratory to investigate interactions between Müller cells and RPE cells.

A final explanation for glial migration beyond the ELM is that Müller cell activation disrupts their binding to photoreceptors and stimulates migration. DAPI$^+$ nuclei within glial membranes suggest that proliferation may also be stimulated. These membranes appear to be primarily glial processes. Müller cells anterior to the atrophic area expressed GFAP and appeared to have reduced GS expression, two hallmarks of activation.[31,32] Reduced GS levels, and other alterations to Müller cell metabolism, were recently reported in AMD retinas.[18] The activation of glia would also explain the formation of glial blooms and membranes on the vitreoretinal surface.[10] In eyes with GA, there was no correlation between the size of the atrophic area and the amount of preretinal glia. Therefore, the pathways involved in pre- and subretinal glial membranes may not be identical.

Subretinal membranes resemble glial scars described elsewhere in the central nervous system. While glial scars are common in many nervous system diseases, it is not yet understood whether they are beneficial or detrimental. In the acute response to injury, activated glial cells release cytokines and neuroprotective agents that may assist in neuronal recovery and regeneration.[33–35] They also phagocytose cell debris and dangerous serum proteins.[33,36,37] Chronic activation of glial cells can also trigger the inflammatory cascade, increase vascular permeability, and disrupt the blood retinal/brain barrier.[33,38–40] Activation also alters water and ion buffering capabilities of Müller cells.[33,41–43] Subretinal glial membranes may create an unhealthy environment for surviving photoreceptor cells and RPE cells. Müller cell activation and membrane formation may also affect neighboring neuronal elements such as neurites of Henle's fiber layer.

The glial membranes in GA eyes reported herein have implications for future clinical practice. These membranes likely provide a barrier, in place of the ELM, that prevents the flow of unwanted materials into or out of the retina. If this membrane is in fact a glial scar as observed elsewhere in the central nervous system, it may impede axon regeneration.[44] This barrier could also make the therapeutic transplantation of photoreceptor cells into the retina very difficult. The loss of linear morphology in Müller cells further complicates the possibility of transplanting cells into the retina. It is important that researchers investigate whether Müller cells regain their linear morphology and metabolic integrity after photoreceptor cell transplantation. Müller cells also produce VEGF and this production is increased upon activation.[45–48] This production of VEGF could further stress photoreceptors and RPE cells at the atrophic border. This VEGF may also explain how some choroidal vessels survive in areas without RPE cells.[15,49] Vascular endothelial growth factor in subretinal glia could also stimulate peripheral choroidal neovascularization as is often observed in donors with GA.[50]

Investigative Ophthalmology & Visual Science

The extension of Müller cell processes from their normal position within the retina indicates their remodeling in disease. Such remodeling likely disrupts the integrity of the ELM, altering the milieu of both the subretinal space and retina. Müller cell remodeling in GA has been suggested by reports of preretinal glial membranes[6,10,12,51] and also metabolic changes in Müller cells.[18] These Müller cell changes could lead to further RPE and photoreceptor loss.

In conclusion, glial cells, primarily Müller cells, create dense membranes posterior to the ELM in the atrophic areas of eyes with GA. These membranes are unlikely to be detected clinically as they lie very close to the retina. To our knowledge, this is the first characterization and visualization in the flat perspective of subretinal glial membranes in GA. This view clearly demonstrates the membrane's density, which is not appreciated in cross section. While these glial membranes may represent a beneficial Müller cell–Müller cell ELM to compensate for the loss of photoreceptors, they may also prevent the transplant of cells as a therapy for GA. These glial membranes also demonstrate the potential remodeling of Müller cells in GA, which may contribute to further photoreceptor and RPE loss. These membranes require further investigation as they may affect VEGF therapy and cell transplantation studies.

Acknowledgments

The authors thank the donors of the Macular Degeneration Research, a program of the BrightFocus Foundation, for their support of this research. The authors also thank Manasee Gedam and Raj Baldeosingh for technical assistance and are indebted to the families of donors, in particular the Johnson Family, for their generous contribution to science.

Supported by BrightFocus Foundation (MME; Clarksburg, MD, USA), the Wilmer Pooled Professor fund (MME; Baltimore, MD, USA), the Research to Prevent Blindness (unrestricted funds to Wilmer Eye Institute; New York, NY, USA), the Foundation Fighting Blindness (GAL; Columbia, MD, USA), and National Eye Institute/National Institutes of Health EY016151 (GAL), EY01765 (Wilmer Core; Bethesda, MD, USA).

Disclosure: **M.M. Edwards**, None; **D.S. McLeod**, None; **I.A. Bhutto**, None; **R. Grebe**, None; **M. Duffy**, None; **G.A. Lutty**, None

References

1. Halfter W. Disruption of the retinal basal lamina during early embryonic development leads to a retraction of vitreal end feet, an increased number of ganglion cells, and aberrant axonal outgrowth. *J Comp Neurol*. 1998;397:89–104.
2. Reichenbach A, Bringmann A. New functions of Müller cells. *Glia*. 2013;61:651–678.
3. McLeod DS, Grebe R, Bhutto I, Merges C, Baba T, Lutty GA. Relationship between RPE and choriocapillaris in age-related macular degeneration. *Invest Ophthalmol Vis Sci*. 2009;50:4982–4991.
4. McLeod DS, Taomoto M, Cao J, Zhu Z, Witte L, Lutty GA. Localization of VEGF receptor-2 (KDR/Flk-1) and effects of blocking it in oxygen-induced retinopathy. *Invest Ophthalmol Vis Sci*. 2002;43:474–482.
5. Madigan MC, Penfold PL, Provis JM, Balind TK, Billson FA. Intermediate filament expression in human retinal macroglia. Histopathologic changes associated with age-related macular degeneration. *Retina*. 1994;14:65–74.
6. Ramirez JM, Ramirez AI, Salazar JJ, de Hoz R, Trivino A. Changes of astrocytes in retinal ageing and age-related macular degeneration. *Exp Eye Res*. 2001;73:601–615.
7. Sullivan TJ, Lambert SR, Buncic JR, Musarella MA. The optic disc in Leber congenital amaurosis. *J Pediatric Ophthalmol Strabismus*. 1992;29:246–249.
8. Wu KH, Madigan MC, Billson FA, Penfold PL. Differential expression of GFAP in early v late AMD: a quantitative analysis. *Br J Ophthalmol*. 2003;87:1159–1166.
9. Fischer AJ, Reh TA. Müller glia are a potential source of neural regeneration in the postnatal chicken retina. *Nat Neurosci*. 2001;4:247–252.
10. Edwards MM, McLeod DS, Bhutto IA, Villalonga MB, Seddon JM, Lutty GA. Idiopathic preretinal glia in aging and age-related macular degeneration. *Exp Eye Res*. 2016;150:44–61.
11. Edwards MM, Rodriguez JJ, Gutierrez-Lanza R, Yates J, Verkhratsky A, Lutty GA. Retinal macroglia changes in a triple transgenic mouse model of Alzheimer's disease. *Exp Eye Res*. 2014;127:252–260.
12. Foos RY. Vitreoretinal juncture; epiretinal membranes and vitreous. *Invest Ophthalmol Vis Sci*. 1977;16:416–422.
13. Edwards MM, McLeod DS, Grebe R, Heng C, Lefebvre O, Lutty GA. Lama1 mutations lead to vitreoretinal blood vessel formation, persistence of fetal vasculature, and epiretinal membrane formation in mice. *BMC Dev Biol*. 2011;11:60.
14. Lutty GA, Merges C, Threlkeld AB, Crone S, McLeod DS. Heterogeneity in localization of isoforms of TGF-beta in human retina, vitreous, and choroid. *Invest Ophthalmol Vis Sci*. 1993;34:477–487.
15. McLeod DS, Bhutto I, Edwards MM, Silver RE, Seddon JM, Lutty GA. Distribution and quantification of choroidal macrophages in human eyes with age-related macular degeneration. *Invest Ophthalmol Vis Sci*. 2016;57:5843–5855.
16. Sunness JS, Bressler NM, Tian Y, Alexander J, Applegate CA. Measuring geographic atrophy in advanced age-related macular degeneration. *Invest Ophthalmol Vis Sci*. 1999;40:1761–1769.
17. Jones BW, Marc RE. Retinal remodeling during retinal degeneration. *Exp Eye Res*. 2005;81:123–137.
18. Jones BW, Pfeiffer RL, Ferrell WD, Watt CB, Tucker J, Marc RE. Retinal remodeling and metabolic alterations in human AMD. *Front Cellular Neurosci*. 2016;10:103.
19. Marc RE, Jones BW, Watt CB, Strettoi E. Neural remodeling in retinal degeneration. *Prog Retin Eye Res*. 2003;22:607–655.
20. Fisher SK, Lewis GP. Müller cell and neuronal remodeling in retinal detachment and reattachment and their potential consequences for visual recovery: a review and reconsideration of recent data. *Vision Res*. 2003;43:887–897.
21. Hippert C, Graca AB, Barber AC, et al. Müller glia activation in response to inherited retinal degeneration is highly varied and disease-specific. *PLoS One*. 2015;10:e0120415.
22. Jones BW, Pfeiffer RL, Ferrell WD, Watt CB, Marmor M, Marc RE. Retinal remodeling in human retinitis pigmentosa. *Exp Eye Res*. 2016;150:149–165.
23. Sethi CS, Lewis GP, Fisher SK, et al. Glial remodeling and neural plasticity in human retinal detachment with proliferative vitreoretinopathy. *Invest Ophthalmol Vis Sci*. 2005;46:329–342.
24. Wickham L, Sethi CS, Lewis GP, Fisher SK, McLeod DC, Charteris DG. Glial and neural response in short-term human retinal detachment. *Arch Ophthalmol*. 2006;124:1779–1782.
25. Tackenberg MA, Tucker BA, Swift JS, et al. Müller cell activation, proliferation and migration following laser injury. *Mol Vis*. 2009;15:1886–1896.
26. Lewis GP, Chapin EA, Luna G, Linberg KA, Fisher SK. The fate of Müller's glia following experimental retinal detachment: nuclear migration, cell division, and subretinal glial scar formation. *Mol Vis*. 2010;16:1361–1372.

27. Yu WQ, Eom YS, Shin JA, et al. Reshaping the cone-mosaic in a rat model of retinitis pigmentosa: modulatory role of ZO-1 Expression expression in DL-alpha-aminoadipic acid reshaping. *PLoS One*. 2016;11:e0151668.
28. Litts KM, Messinger JD, Dellatorre K, Yannuzzi LA, Freund KB, Curcio CA. Clinicopathological correlation of outer retinal tubulation in age-related macular degeneration. *JAMA Ophthalmol*. 2015;133:609–612.
29. Schaal KB, Freund KB, Litts KM, Zhang Y, Messinger JD, Curcio CA. Outer retinal tubulation in advanced age-related macular degeneration: optical coherence tomographic findings correspond to histology. *Retina*. 2015;35:1339–1350.
30. Johnson PT, Lewis GP, Talaga KC, et al. Drusen-associated degeneration in the retina. *Invest Ophthalmol Vis Sci*. 2003; 44:4481–4488.
31. Bringmann A, Grosche A, Pannicke T, Reichenbach A. GABA and glutamate uptake and metabolism in retinal glial (Müller) cells. *Front Endocrinol*. 2013;4:48.
32. Nakazawa T, Takeda M, Lewis GP, et al. Attenuated glial reactions and photoreceptor degeneration after retinal detachment in mice deficient in glial fibrillary acidic protein and vimentin. *Invest Ophthalmol Vis Sci*. 2007;48:2760–2768.
33. Bringmann A, Iandiev I, Pannicke T, et al. Cellular signaling and factors involved in Müller cell gliosis: neuroprotective and detrimental effects. *Prog Retin Eye Res*. 2009;28:423–451.
34. Cao W, Wen R, Li F, Cheng T, Steinberg RH. Induction of basic fibroblast growth factor mRNA by basic fibroblast growth factor in Müller cells. *Invest Ophthalmol Vis Sci*. 1997;38: 1358–1366.
35. Harada T, Harada C, Nakayama N, et al. Modification of glial-neuronal cell interactions prevents photoreceptor apoptosis during light-induced retinal degeneration. *Neuron*. 2000;26: 533–541.
36. Chang ML, Wu CH, Chien HF, Jiang-Shieh YF, Shieh JY, Wen CY. Microglia/macrophages responses to kainate-induced injury in the rat retina. *Neurosci Res*. 2006;54:202–212.
37. Rosenthal AR, Appleton B. Histochemical localization of intraocular copper foreign bodies. *Am J Oophthalmol*. 1975;79:613–625.
38. Cotinet A, Goureau O, Hicks D, Thillaye-Goldenberg B, de Kozak Y. Tumor necrosis factor and nitric oxide production by retinal Müller glial cells from rats exhibiting inherited retinal dystrophy. *Glia*. 1997;20:59–69.
39. Drescher KM, Whittum-Hudson JA. Herpes simplex virus type 1 alters transcript levels of tumor necrosis factor-alpha and interleukin-6 in retinal glial cells. *Invest Ophthalmol Vis Sci*. 1996;37:2302–2312.
40. Yuan L, Neufeld AH. Tumor necrosis factor-alpha: a potentially neurodestructive cytokine produced by glia in the human glaucomatous optic nerve head. *Glia*. 2000;32:42–50.
41. Bringmann A, Pannicke T, Grosche J, et al. Müller cells in the healthy and diseased retina. *Prog Retin Eye Res*. 2006;25:397–424.
42. Lewis GP, Guerin CJ, Anderson DH, Matsumoto B, Fisher SK. Rapid changes in the expression of glial cell proteins caused by experimental retinal detachment. *American J Ophthalmol*. 1994;118:368–376.
43. Lieth E, Barber AJ, Xu B, et al. Glial reactivity and impaired glutamate metabolism in short-term experimental diabetic retinopathy. Penn State Retina Research Group. *Diabetes*. 1998;47:815–820.
44. McGraw J, Hiebert GW, Steeves JD. Modulating astrogliosis after neurotrauma. *J Neurosci Res*. 2001;63:109–115.
45. Aiello LP, Avery RL, Arrigg PG, et al. Vascular endothelial growth factor in ocular fluid of patients with diabetic retinopathy and other retinal disorders. *N Engl J Med*. 1994; 331:1480–1487.
46. Eichler W, Kuhrt H, Hoffmann S, Wiedemann P, Reichenbach A. VEGF release by retinal glia depends on both oxygen and glucose supply. *Neuroreport*. 2000;11:3533–3537.
47. Eichler W, Yafai Y, Wiedemann P, Reichenbach A. Angiogenesis-related factors derived from retinal glial (Müller) cells in hypoxia. *Neuroreport*. 2004;15:1633–1637.
48. Yafai Y, Iandiev I, Wiedemann P, Reichenbach A, Eichler W. Retinal endothelial angiogenic activity: effects of hypoxia and glial (Müller) cells. *Microcirculation*. 2004;11:577–586.
49. Seddon JM, McLeod DS, Bhutto IA, et al. Histopathological insights into choroidal vascular loss in clinically documented cases of age-related macular degeneration. *JAMA Ophthalmol*. 2016;134:1272–1280.
50. Sunness JS, Gonzalez-Baron J, Bressler NM, Hawkins B, Applegate CA. The development of choroidal neovascularization in eyes with the geographic atrophy form of age-related macular degeneration. *Ophthalmology*. 1999;106:910–919.
51. Foos RY. Vitreoretinal juncture–simple epiretinal membranes. *Albrecht Von Graefes Arch Klin Exp Ophthalmol*. 1974;189: 231–250.

Investigative Ophthalmology & Visual Science